Hemiacetal-Based Dynamic Systems: A New Mechanistic Insight

Radek Coufal*[1,2], Zdeněk Tošner[3], Dušan Drahoňovský[4] and Jiří Vohlídal[1]

[1]*Department of Physical and Macromolecular Chemistry, Faculty of Science, Charles University, Hlavova 8/2030, 128 40 Prague 2, Czech Republic*

[2]*Department of Science and Research, Faculty of Health Studies, Technical University of Liberec, Studentská 1402/2, 461 17 Liberec 1, Czech Republic*

[3]*NMR Laboratory, Faculty of Science, Charles University, Hlavova 8/2030, 128 40 Prague 2, Czech Republic*

[4]*Department of Organic Chemistry, Faculty of Science, Charles University, Hlavova 8/2030, 128 40 Prague 2, Czech Republic*

†*Not among us*

Supporting Information

TABLE OF CONTENTS

General. NMR spectra were recorded on VNMRS300, VarianUNITY INOVA 400, and Bruker AVANCE-III 600 spectrometers. ^{1}H NMR and ^{13}C NMR spectra are referenced to residual solvent signal. High-resolution mass spectra were obtained with Q-Tof micro (Waters) spectrometer. IR spectra were recorded on Nicolet Avatar 370 FT-IR using KBr-diluted samples and diffuse reflectance technique (DRIFT). Crystallographic data were collected on Nonius Kappa CCD diffractometer equipped with Bruker Apex-II CCD detector and a Cryostream Cooler (Oxford Instruments) at 150(2) using graphite-monochromated Mo Kα radiation (λ = 0.71073 Å). The crystal structure was solved by direct methods (SHELXS),[1] and the structure model was refined by full matrix least squares based on F^2 (SHELXL2018).[2] The non-hydrogen atoms were refined with anisotropic displacement parameters. The hydrogen atoms residing on the oxygen atoms were identified on the difference electron density maps and refined as riding atoms with U_{iso}(H) set to 1.2-times U_{eq}(O). Hydrogen atoms residing on the carbon atoms were included in their theoretical positions and refined analogously. Geometric data as well as structural drawings were obtained with a recent version of the PLATON progam.[3] Melting points were measured on Büchi Melting Point B-545 (±0.2 °C). A radial-layer chromatograph (Chromatotron^{TM}) was used for purification of crude products. Molecular sieves (3Å, powder, Alfa Aesar) were heated at ca. 180 °C under reduced pressure for several hours prior to use. Cesium fluoride (Fluorochem) was dried by heating at ca. 180 °C under reduced pressure. Anhydrous alcohols (Sigma-Aldrich) were used as received. Tetrahydrofuran (THF) and dimethoxyethane (DME) were distilled from sodium/benzophenone ketyl under argon atmosphere. Dichloromethane (DCM) was distilled from CaH_2 under argon atmosphere. Other solvents (for workup and chromatography) and chemicals obtained from commercial suppliers were used without any further purification.

Synthesis

Methyl pyrazinoate. This compound was prepared by a modification of the procedures of Goodson and Bark.[4] 2-Pyrazine carboxylic acid (25.70 g; 207 mmol) was suspended in dry MeOH (250 mL) and concentrated H_2SO_4 (ca. 10 drops) was added. The mixture was heated to reflux for 2 days. After cooling to ambient temperature, the solution was treated with solid $NaHCO_3$ (5 g) for 16 h. The mixture was concentrated under reduced pressure, filtered, and the residue was diluted with DCM. After drying over $MgSO_4$, the solution was filtered through alumina column. The solvent was removed under reduced pressure, and the residue was sublimed in vacuo (ca. 110 °C) to give 20.9 g (73 %) of the title compound as a white

crystalline solid. ^{1}H NMR (299.94 MHz, $CDCl_3$): δ = 9.34 (d, 1H, pz, ^{4}J = 1.5 Hz), 8.80 (d, 1H, pz, ^{3}J = 2.4 Hz), 8.74 (dd, 1H, pz, ^{3}J = 2.4 Hz, ^{4}J = 1.5 Hz), 4.06 (s, 3H, CH_3) ppm. ^{13}C NMR (75.4 Hz, $CDCl_3$): δ = 164.5 (C=O), 147.9 (pz-H), 146.4 (pz-H), 144.5 (pz-H), 143.4 (pz-C), 53.3 (CH_3) ppm.

***O*-Silyl ether hemiacetal.** Methyl pyrazinoate (200.0 mg; 1.45 mmol) was dissolved in a mixture of DCM/DME (2.3 mL, 7:1), and freshly dried CsF (12.2 mg; 79 µmol) was added under argon atmosphere. Then, TMS-CF_3 (0.28 mL; 1.84 mmol) was slowly added under argon atmosphere (argon-vacuum cycles) by microsyringe, where the reaction mixture turned brown-orange. The reaction was monitored by TLC (silicagel, DCM/hexane 1:1 or pure DCM). The reaction mixture was stirred for 70 min, and then the reaction was quenched using H_2O (5 mL), and aqueous phase was extracted with DCM (3 × 20 mL). The combined organic layers were dried over $MgSO_4$ (1.8 g), concentrated under reduced pressure to dryness, and the residue was dried in vacuo to afford 336.3 mg (83 %) of the product as a orange-brown viscous oil. The product was further purified by radial TLC (silicagel, DCM/hexane 1:1 – DCM) to finally afford 227.2 mg (56 %) of a colorless viscous oil. ^{1}H NMR (600.17 MHz, CD_2Cl_2): δ = 8.95 (d, 1H, pz, ^{4}J = 1.2 Hz), 8.63 (dd, 1H, pz, ^{3}J = 2.7 Hz, ^{4}J = 1.2 Hz), 8.62 (d, 1H, pz, ^{3}J = 2.7 Hz), 3.32 (s, 3H, OCH_3), 0.25 (s, 9H, OTMS) ppm. ^{13}C NMR (150.91 MHz, CD_2Cl_2): δ = 150.7 (pz-C), 146.0 (pz-H), 145.8 (pz-H), 143.8 (pz-H), 122.9 (k, CF_3, J_{CF} = 290.2 Hz), 98.0 (k, **C**-CF_3, $^{2}J_{CF}$ = 31.7 Hz), 51.6 (OCH_3), 1.5 (OTMS) ppm. ^{19}F NMR (282.19 MHz, CD_2Cl_2): δ = −80.3 (s) ppm. IR (KBr): 3081 (vw), 3052 (vw), 2959 (w), 2899 (vw), 2848 (vw), 1473 (vw), 1440 (vw), 1401 (w), 1311 (w), 1293 (w), 1260 (m), 1180 (vs), 1135 (s), 1105 (s), 1060 (w), 1021 (w), 997 (w), 967 (w), 890 (m), 851 (s), 821 (w), 761 (w), 719 (w), 641 (w), 414 (w) cm^{-1}. HRMS (APCI): calc. for $C_{10}H_{16}N_2O_2F_3Si$ ($[M+H]^+$) 281.0933, found 281.0930.

Hydrate (Hy). To a solution of *O*-silyl ether hemiacetal (95.3 mg; 0.34 mmol) in THF (2.5 mL) AcOH (99%, 0.19 mL) and KF (28.7 mg, 0.49 mmol) in H_2O (0.2 mL) were added. The reaction mixture was allowed to stir at r. t. under argon atmosphere. The reaction was monitored by TLC (silicagel, DCM, mini-workup using sat. $NaHCO_3$). After 75 min, sat. $NaHCO_3$ (5 mL) was added and THF was removed under reduced pressure. Aqueous phase was extracted with EtOAc (4 × 10 mL) and the combined organic layers were dried over $MgSO_4$ (2.1 g). After concentration under reduced pressure, the resulting residue was dried in vacuo to afford 56.5 mg (86 %) of a colorless solid. For further use it was purified by radial

TLC (silicagel, hexane/EtOAc 4:3) to finally afford 32.3 mg (49 %) of a colorless crystalline solid. Trituration of the residue with DCM/hexane (1:1) was also approved for purification purpose. ^{1}H NMR (600.17 MHz, CD_3CN): δ = 9.02 (s, 1H, pz), 8.74 (d, 1H, pz, ^{3}J = 2.4 Hz), 8.63 (dd, 1H, pz, ^{3}J = 2.4 Hz, ^{4}J = 1.2 Hz), 5.93 (s, 2H, OH) ppm. ^{13}C NMR (150.91 MHz, CD_3CN): δ = 150.6 (pz-C), 147.3 (pz-H), 145.2 (pz-H), 143.8 (pz-H), 124.0 (k, CF_3, J_{CF} = 287.2 Hz), 93.0 (k, **C**-CF_3, $^{2}J_{CF}$ = 32.6 Hz) ppm. ^{19}F NMR (282.19 MHz, CD_3CN): δ = −84.4 (s) ppm. IR (KBr): 3351 (b), 3102 (w+b), 3040 (b), 2866 (w+b), 2836 (w+b), 2717 (w+b), 2528 (w+b), 1473 (w), 1416 (w), 1401 (w), 1389 (w), 1296 (w), 1278 (s), 1236 (m), 1210 (m), 1168 (vs), 1144 (m), 1126 (m), 1078 (s), 1054 (s), 1021 (m), 958 (w), 937 (m), 860 (m), 812 (w), 767 (w), 719 (w), 662 (w), 611 (w), 576 (w), 423 (m) cm^{-1}. HRMS (APCI): calc. for $C_6H_4N_2OF_3$ ($[M-H_2O+H]^+$) 177.0276, found 177.0268. M. p. 86.9 °C. Single crystal for X-ray analysis was obtained by slow diffusion of chloroform into the solution of the title compound in THF at r. t.

Hemiacetalization and hydration experiments

Preparation of samples. The stock solutions for NMR **hemiacetalization experiments** were prepared (just before use) by weighing (± 0.1 mg) into a 1mL volumetric flask of the hydrate and by using appropriate microsyringe for alcohols, followed by addition of CD_3CN to form solutions of 0.1M and 1M, respectively, and 1 mL total. Then, the solution of respective alcohol (1-butanol: 0.09 mL; 90 μmol, benzyl alcohol: 0.12 mL; 120 μmol, 2-methoxyethanol: 0.18 mL; 180 μmol, 2-propanol: 0.18 mL; 180 μmol) was added to the solution of the hydrate (0.3 mL; 30 μmol) in 1mL volumetric flask using microsyringe, followed by addition of CD_3CN to make 1 mL total (different hydrate/alcohol ratios were used in order to generate approximately equal proportions of the hemiacetals in the dynamic systems, *vide infra*). After, molecular sieve (3Å, ca. 50 mg) and magnetic stirrer were added and the mixture was allowed to stir for ca. 3 h at room temperature. Molecular sieve was filtered off using PTFE syringe filter, the solution was added to fresh portion of molecular sieve (ca. 50 mg) in a small vial and the mixture was stirred overnight under argon atmosphere. Finally, the filtered solution was transferred to NMR tube, which was filled with argon and kept airtight throughout spectra acquisition.

Sample for the **hydration experiment** was prepared as follows: The hydrate (3.3 mg; 17 μmol) in NMR tube under argon atmosphere was dissolved in CD_3CN (stored in the

presence of 3Å molecular sieve under argon atmosphere) and the sample was kept in desiccator with silicagel overnight.

The experiment comprising the **simultaneous presence of 1-butanol and benzyl alcohol** was prepared as follows: The stock solutions were prepared by weighing into a 1mL volumetric flask of the hydrate and by using microsyringe for the alcohols, followed by addition of CD_3CN to form solution of 0.05M and 0.5M, respectively, and 1mL total. Then, the solution of benzyl alcohol (0.09 mL; 45 μmol) was added to the solution of the hydrate (0.6 mL; 30 μmol) in NMR tube using microsyringe, followed by gradual addition of the solution of 1-butanol (0.09 mL; 45 μmol). Sample was equilibrated at r. t. followed by addition to molecular sieve (3Å) and CD_3CN (0.1 mL) in a small vial and the mixture was allowed to equilibrate overnight. Finally, the filtered solution was transferred to NMR tube, and the sample was kept under argon atmosphere.

Measurments and spectra analysis. ^{1}H and ^{19}F NMR spectra were recorded on VNMRS300, VarianUNITY INOVA 400 and Bruker AVANCE-III 600 (for the mixed alcohol system) spectrometers, soon after samples preparation. Samples were equilibrated at particular temperature for ca. 20 min before the acquisition started. For each peak in ^{19}F NMR spectrum three proper integrations were made, and the average values of relative amount of the hemiacetal at equilibrium y and of ratio h/k were used in subsequent equilibrium constant calculation for the hemiacetal formation, in accordance with Eqn (1):

$$K = h / k\,([\mathrm{ROH}]_{tot} - y\,[\mathrm{K}]_{tot}) \quad (1)$$

where h and k are the integrals for [H] and [K], respectively and $[K]_{tot}$ is total concentration of the ketone and its hydrate.

Similar approach was applied for the hydration equilibrium, where the water content was determined by integration in ^{1}H NMR spectra. Equilibrium constant of the hydration was used for the calculation of free water content in 1D-EXSY experiments to determine the hydration equilibrium.

The determination of equilibrium constants was accomplished at 5 temperatures in the range of −10 °C - 45 °C. Thermodynamic parameters were calculated based on the van´t Hoff plots (for the hydration and single alcohol experiments, see **Figure S2**), where the linear fitting treatment of the data gave the values of adj. R^2 better than 0.990. Since ^{19}F NMR has

several advantages, e. g., signals are well separated without splitting, has almost the same sensitivity like ^{1}H NMR (moreover, there are three fluorine atoms providing singlet peak), the integrations were performed in ^{19}F NMR spectra in each case. The obtained results can be, however, checked following the integration in ^{1}H NMR spectra, which yields the values of $\Delta_r G_{int}$ with difference at most to about ± 1 kJ/mol.

1D-EXSY. Since our systems fulfill feasibility criteria, i.e., interconversion of two sites is slow on the ^{19}F chemical shift time scale (resulted in well separated signals) and the relaxation time T_1 of the spin in each state in not much shorter than the lifetime of the existing states, the magnetization transfer of the involved sites can be analyzed by plotting the normalized intensity of the build-up peak against mixing time yielding the build-up curve. The intensity of the excited peak is extrapolated to zero mixing time, and this value is used to normalize the intensity of the build-up peak. Different delays up to 1 s were used and the longest values gave up to 6% and 25% of transferred magnetization for single and mixed alcohol systems, respectively. The build-up curve is then fitted with a second-order polynomial function, and the first derivative at time zero is used as the effective exchange rate (k_{fwd} or k_{bwd}, for forward or backward process, respectively). The reaction rate constants k_1 and k_{-1} are solved individually (in two separate experiments, where the resonance of either the ketone or of the hemiacetal and hydrate, respectively, are selectively excited) by the formula $k_{fwd} = [ROH]k_1$ and $k_{bwd} = k_{-1}$, where k_{fwd} and k_{bwd} correspond to the experimentally measured build-up rates for NMR signal for forward and backward processes, respectively, and [ROH] denotes the concentration of the free alcohol. Using the rate constants, the association constants ($K = k_1/k_{-1}$) and the values of $\Delta_r G$ ($\Delta_r G = -RTlnK$) could be calculated and compared with those determined from the van´t Hoff plots.

Table S1 Equilibrium compositions (%) of **R**-systems based on ^{19}F NMR (298 K).

R-system	K	Hy	H
H	11.8	88.2	
Bu	9.1	10.2	80.7
Bn	15.3	10.0	74.7
2-ME	5.3	25.5	69.2
i-Pr	18.3	4.0	77.7

Computational Details. All structures employed in this study were optimized using the M06-2X functional[5] in conjunction with the 6-311++G(d,p) basis set, as implemented in the Gaussian 09 program package.[6] Frequency analyses at the same level of theory were performed in all the stationary geometries in order to assign them as genuine minima (no imaginary frequency) or transition states (TS, only one imaginary frequency corresponding to the reaction coordinate) on the potential energy surface (PES) as well as to evaluate the thermochemical corrections at 298.15 K. A pruned (99, 590) UltraFine grid was used for the numerical computation of two electron-integrals. The connectivity of each TS with the associated minima was described using IRC (intrinsic reaction coordinate) procedure.[7] For stationary points a detailed conformational analysis was carried out. Relaxed PES scan was performed for C–O–C–O and N–C–C–O torsion angels, starting from the optimized minima following the IRC. Angles were varied from −180° to +180° with step size 6° and geometrical structures with the lowest electronic energy found at PES were subsequently reoptimized. The solvent effects were estimated through the SMD model[8] in acetonitrile as the continuum dielectric (ε = 35.688) within reoptimalization of the located stationary points at the same level of theory. Analytical Hessians were again calculated to control the identity of the stationary points as well as to obtain the thermochemical corrections at 298.15 K. Within implicit-explicit model, one or two acetonitrile molecules were added to stationary points and this explicit subsystem was optimized using SMD. Here, for all systems the same procedure was applied (starting from analogical solvent-solute geometries) and we did not use any conformational solvent-solute sampling. Corrections for basis set superposition error (BSSE) were not included. The counterpoise method[9] applied for the water-assisted hydration yields BSSE energies of 10.3 and 5.0 kJ/mol for the pre-RC and post-RC, respectively. The final energy diagrams were obtained by calculating solution phase free energies according to Eqn (1):

$$G_{soln} = E_{gas} + G_n + \Delta G_{solv} + 1.89 \text{ kcal mol}^{-1} \qquad (1)$$

where G_{soln} refers to solution phase free energy, E_{gas} refers to electronic energy obtained in the single point calculations at M06-2X in conjunction with the def2-TZVPPD basis set[10], G_n refers to thermal correction to Gibbs free energy obtained at M06-2X/6-311++G(d,p) level and ΔG_{solv} is solvation free energy obtained as a difference $G_{soln} - G_{gas}$ at M062X/6-311++G(d,p) level, where G_{gas} is gas phase free energy. The final term 1.89 kcal mol^{-1}

converts from the gas-phase standard state (defined by T and P) to the solution-phase standard state of 1 M.

The most stable geometrical structures of the alcohols are in agreements with the literature.[11]

Gas-phase results

Table S2 Relative Gibbs free energies, in kJ/mol, with respect to the sum of the isolated reactants of the transition states TS1 and the respective pre-RC1 complexes for the hydration and hemiacetalization of the ketone. **R** indicates the reacting molecule **R**OH.

R	**pre-RC1**	**TS1**
H	11.8	180.1
Bu	14.7	162.0
Bn	12.4	159.4
2-ME	22.1	175.2
i-Pr	17.1	158.4

Table S3 Relative Gibbs free energies, in kJ/mol, with respect to the sum of the isolated reactants of key intermediates (the pre-reactive complex (pre-RC), transition state (TS), and post-reactive complex (post-RC)), and the hydrate (**Hy**) for the water- and alcohol-assisted hydration. **R** indicates the assisting molecule **R**OH.

R	**pre-RC**	**TS**	**post-RC**	**Hy**
H	17.0	99.5	−24.9	
Bu	19.0	94.2	−26.3	
Bn	20.9	83.4	−19.8	−24.5
2-ME	20.9	101.5	−26.2	
i-Pr	17.2	92.2	−25.2	

Table S4 Relative Gibbs free energies, in kJ/mol, with respect to the sum of the isolated reactants of key intermediates (the pre-reactive complexes (pre-RC2 and pre-RC3 connected with TS2 and TS3, respectively), water-assisted transition state (TS2), alcohol-assisted transition state (TS3), and post-reactive complexes (post-RC2 and post-RC3 connected with TS2 and TS3, respectively), and the hemiacetals (H-R) for the hemiacetalization of the ketone. **R** indicates the reacting (for the TS3 simultaneously assisting) alcohol **R**OH.

R	**pre-RC2**	**pre-RC3**	**TS2**	**TS3**	**post-RC2**	**post-RC3**	**H-R**
Bu	16.4	17.6	97.3	89.9	−2.5	−0.3	−28.9
Bn	12.1	19.3	92.3	89.4	−11.2	−6.9	−28.0
2-ME	19.9	24.3	98.0	99.8	−8.9	0.7	−19.3
i-Pr	17.3	20.5	94.4	88.5	−5.5	−4.2	−26.1

Table S5 Relative Gibbs free energies, in kJ/mol, with respect to the sum of the isolated reactants of key intermediates (the pre-reactive complex (pre-RC3), post-reactive complex (post-RC3) connected with alcohol-assisted transition state (TS3) for the hemiacetalization of the ketone in the simultaneous presence of BuOH and BnOH. $\mathbf{R_1}$ and $\mathbf{R_2}$ indicate the reacting alcohol $\mathbf{R_1}$OH and assisting alcohol $\mathbf{R_2}$OH, respectively.

$\mathbf{R_1}$	$\mathbf{R_2}$	pre-RC3	TS3	post-RC3
Bu	Bn	24.6	94.7	0.4
Bn	Bu	18.5	86.1	−8.4

Table S6. Relative Gibbs free energies, in kJ/mol, with respect to the sum of the isolated reactants of key intermediates (the pre-reactive complexes (pre-RC4 connected with TS4), N-assisted transition state (TS4), post-reactive complexes (post-RC4 connected with TS4) for the hydration and hemiacetalization of the ketone. **R** indicates the reacting molecule **R**OH.

R	pre-RC4	TS4	post-RC4
H	11.8	135.2	124.4
Bu	14.2	121.8	119.8
Bn	18.1	114.6	107.3
2-ME	19.6	115.2	105.8
i-Pr	16.5	122.1	119.6

Table S7. Relative Gibbs free energies, in kJ/mol, with respect to the sum of the isolated reactants of the transition state **TS5** (transition state for rotation of pyrazine ring in zwitterionic post-reactive complexes post-RC4) in gas phase and bulk solvent.

R	GAS	SMD
H	139.4	88.2
Bu	138.9	88.8
Bn	121.1	89.4
2-ME	119.4	79.9
i-Pr	137.0	92.2

Table S8. Relative Gibbs free energies (SMD), in kJ/mol, with respect to the sum of the isolated reactants of key intermediates (the pre-reactive complexes (pre-RC4 connected with TS4), N-assisted transition state (TS4), post-reactive complexes (post-RC4 connected with TS4) for the hydration of the ketone regarding 0-2 explicit ACN molecules.

n Explicit Molecules	**pre-RC4**	**TS4**	**post-RC4**
0	12.4	109.9	74.3
1	22.4	114.4	79.4
2	18.9	110.2	79.5

X-ray structure data

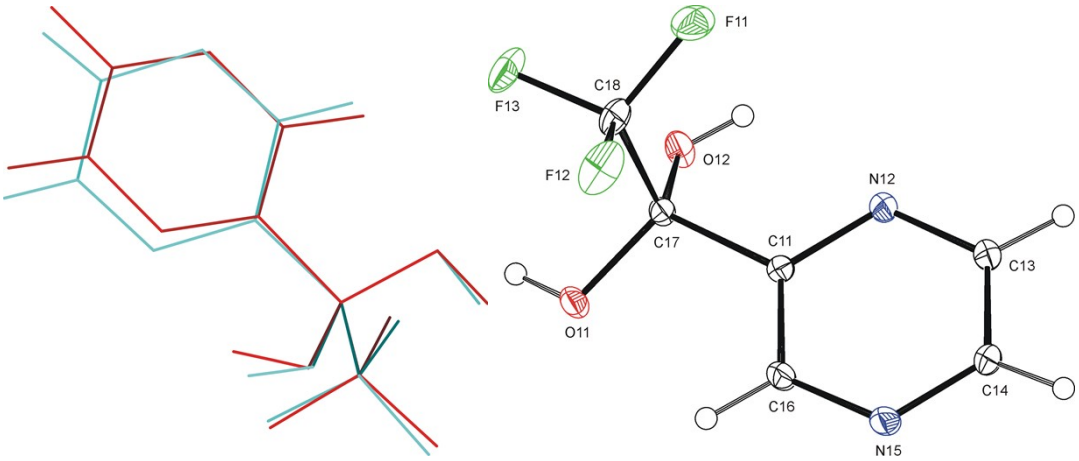

Figure S1 Left: Comparison of independently DFT calculated (gas phase, red) and experimentally determined (X-ray, blue) geometries for the hydrate. Right: ORTEP presentation of solid state structure of the hydrate.

Detailed crystallographic data for the hydrate have been deposited at the Cambridge Crystallographic Data Centre, CCDC no. 1902217. Copy of this information may be obtained free of charge from the director, CCDC, 12 Union Road, Cambridge CB2 1EY, UK (http://www.ccdc.cam.ac.uk; fax: +44-1223-336033; e-mail: deposit@ccdc.cam.ac.uk).

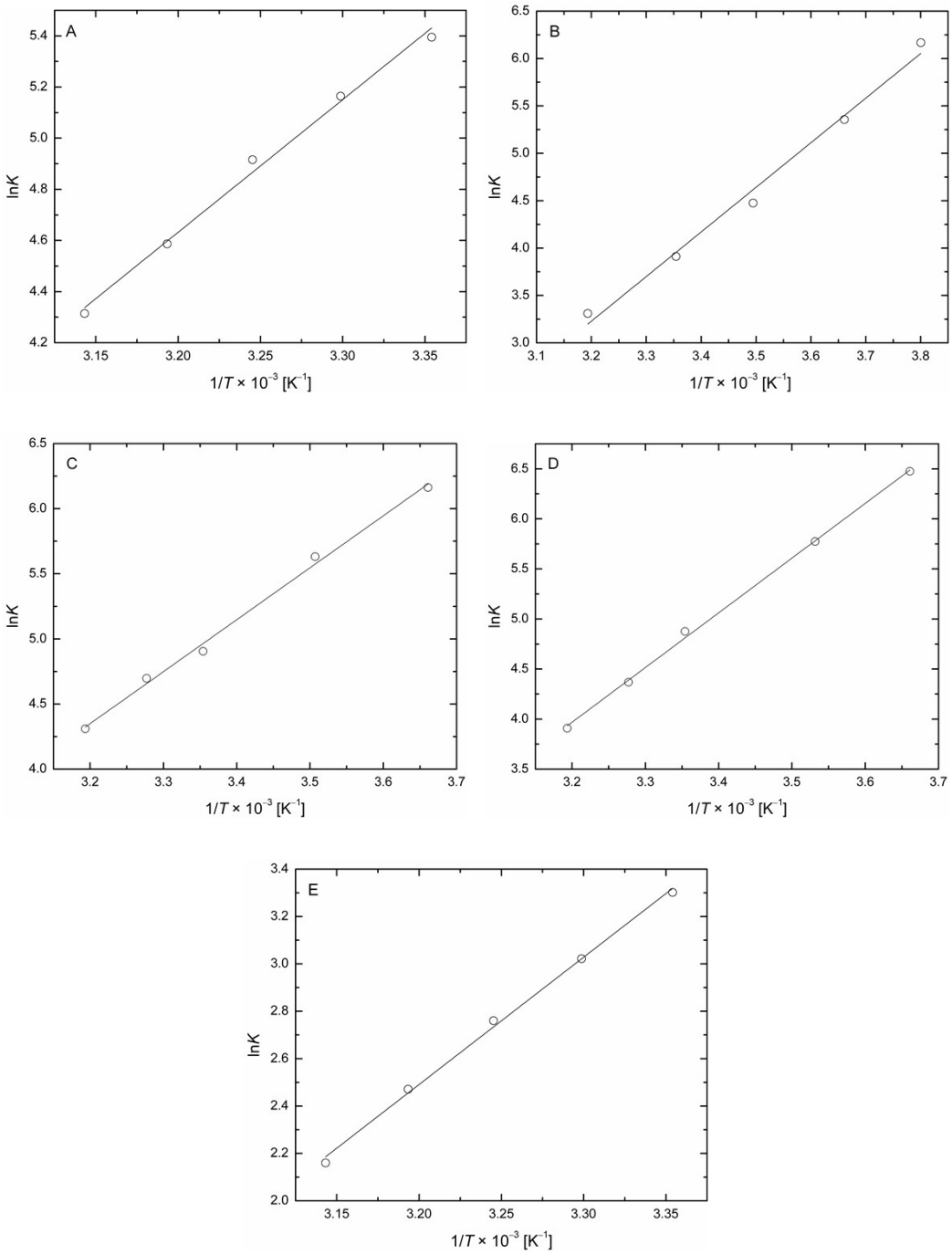

Figure S2 Van´t Hoff plots of (A) the hydration and hemiacetalization reactions of the ketone with (B) benzyl alcohol, (C) 1-butanol, (D) 2-methoxyethanol, (E) 2-propanol

EXSY Build up curves

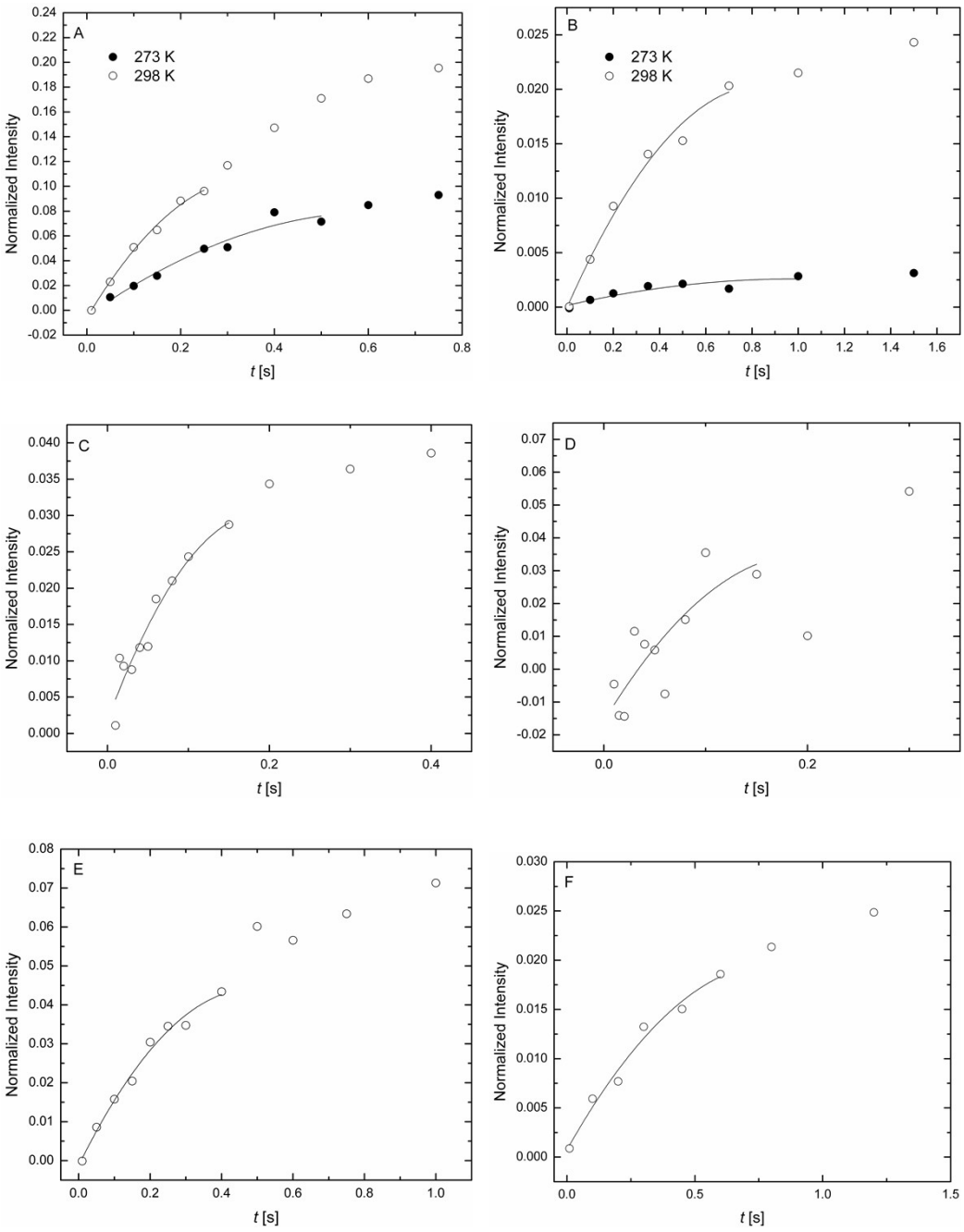

Figure S3 Build-up curves of the signal from (A) 2-methoxyethyl hemiacetal, when the ketone excited selectively; (B) ketone, when 2-methoxyethyl hemiacetal excited selectively; (C) the hydrate, when ketone excited selectively (in the presence of BnOH); (D) ketone, when hydrate excited selectively (in the presence of BnOH); (E) hydrate, when ketone excited selectively (in the presence of 2-MEOH), and (F) ketone, when hydrate excited selectively (in the presence of 2-MEOH). Fit of the initial buildup to a second-order polynomial is depicted by the solid line. For (C), (D), (E), and (F): T = 298 K.

^{1}H NMR and ^{19}F NMR spectra

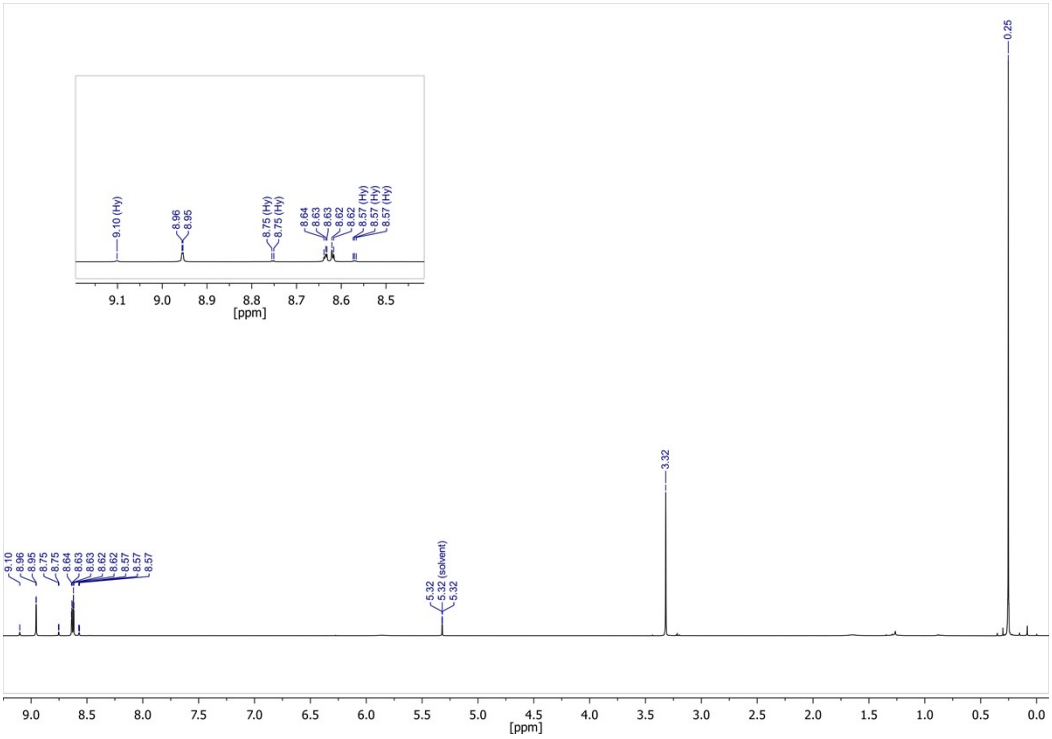

Figure S4 ^{1}H NMR spectrum (298 K) of *O*-silylether hemiacetal in CD_2Cl_2. Peaks of the hydrate (Hy) are visible due to the partial desilylation in NMR solvent.

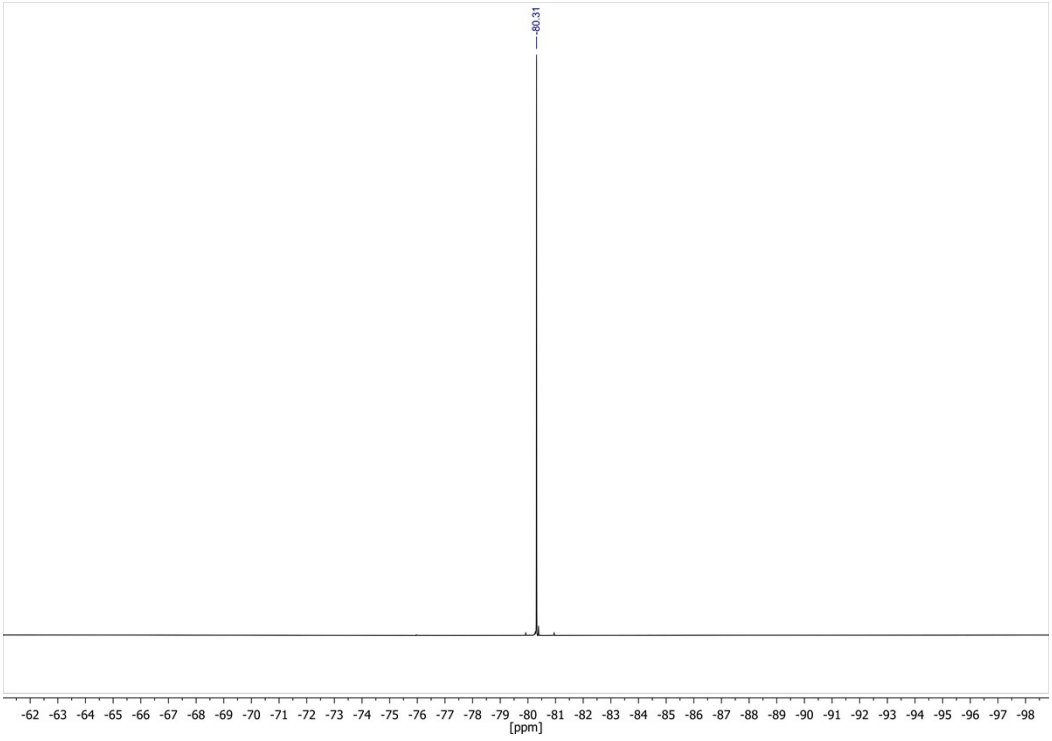

Figure S5 ^{19}F NMR spectrum (298 K) of *O*-silylether hemiacetal in CD_2Cl_2.

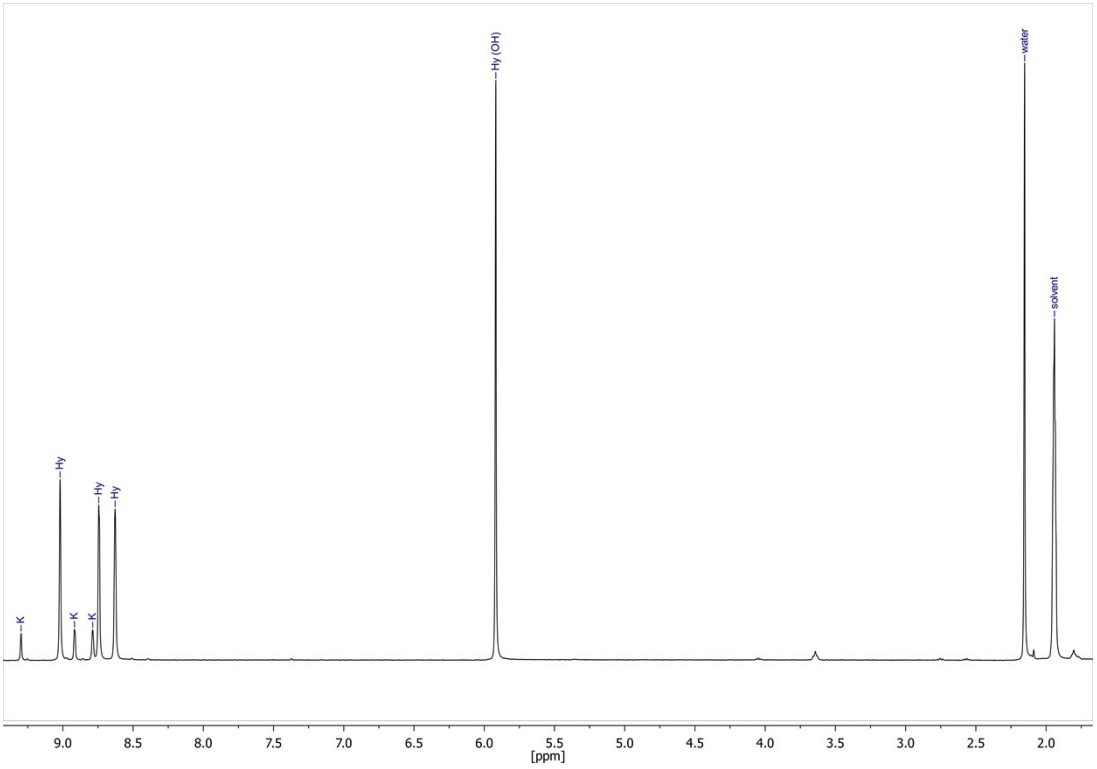

Figure S6 ^{1}H NMR spectrum (298 K) of the hydration in CD_3CN. K = ketone; Hy = hydrate.

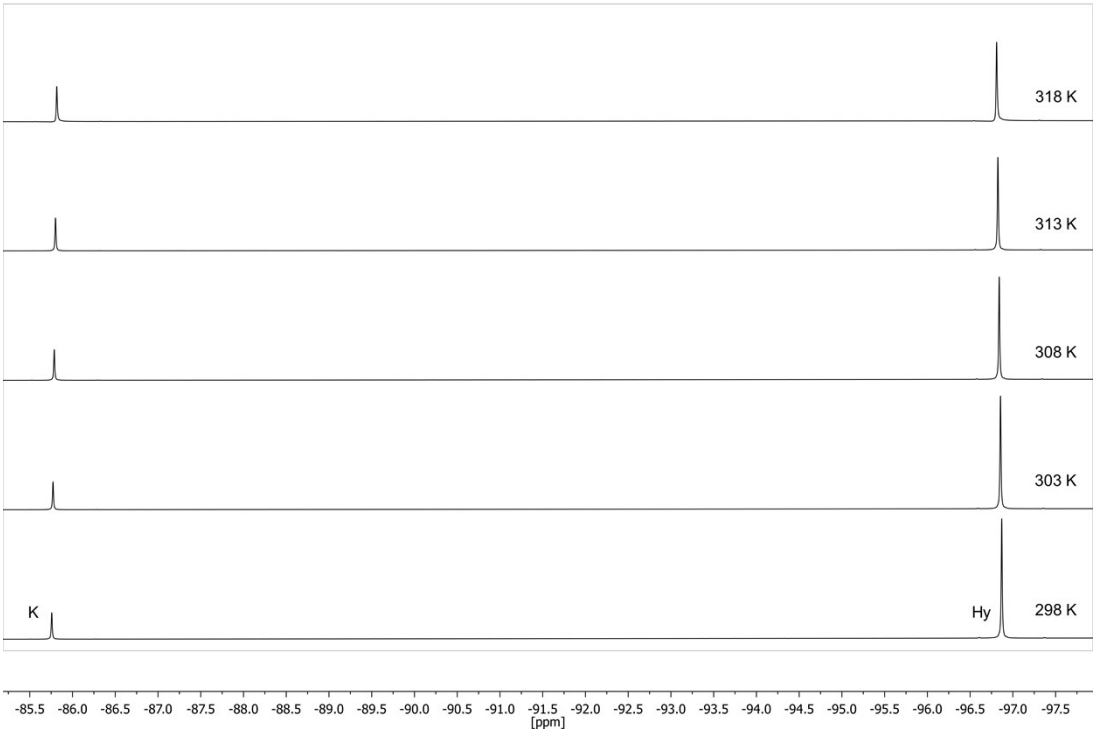

Figure S7 Temperature-dependent ^{19}F NMR spectra of the hydration in CD_3CN. K = ketone; Hy = hydrate.

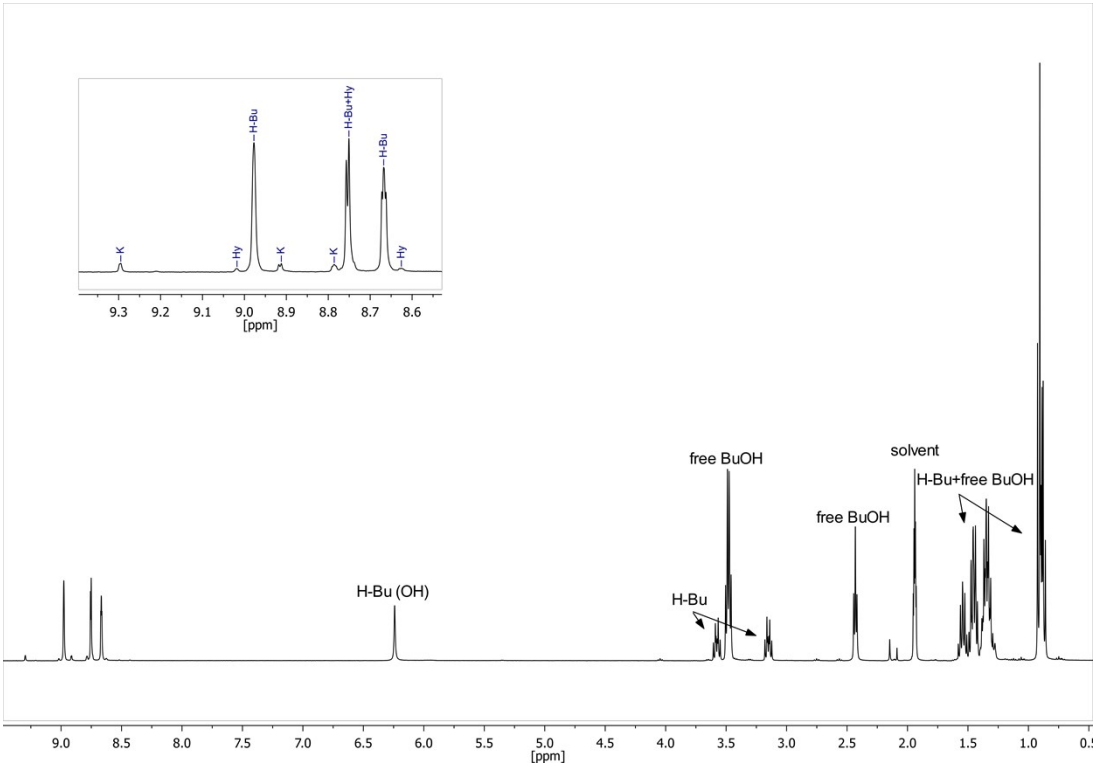

Figure S8 ^{1}H NMR spectrum (298 K) of the H-Bu-dynamic system (using 3 eq. of BuOH) in CD_3CN. H-Bu = butyl hemiacetal; K = ketone; Hy = hydrate.

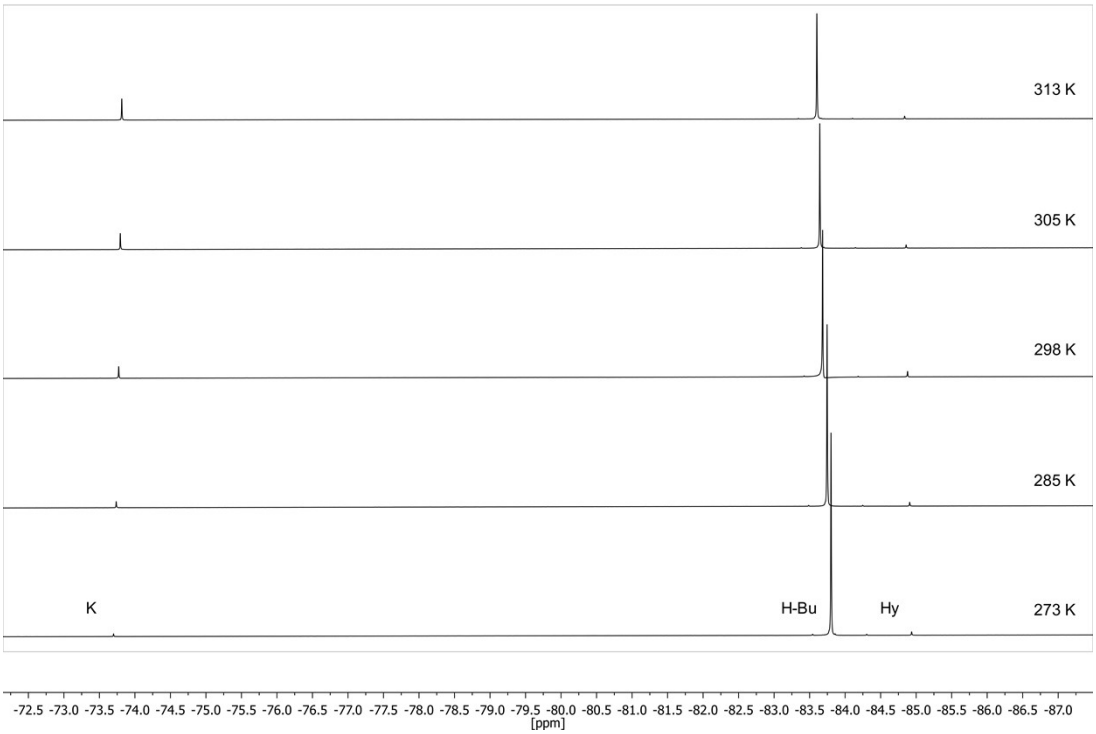

Figure S9 Temperature-dependent ^{19}F NMR spectra of the H-Bu-dynamic system (using 3 eq. of BuOH) in CD_3CN. H-Bu = butyl hemiacetal; K = ketone; Hy = hydrate.

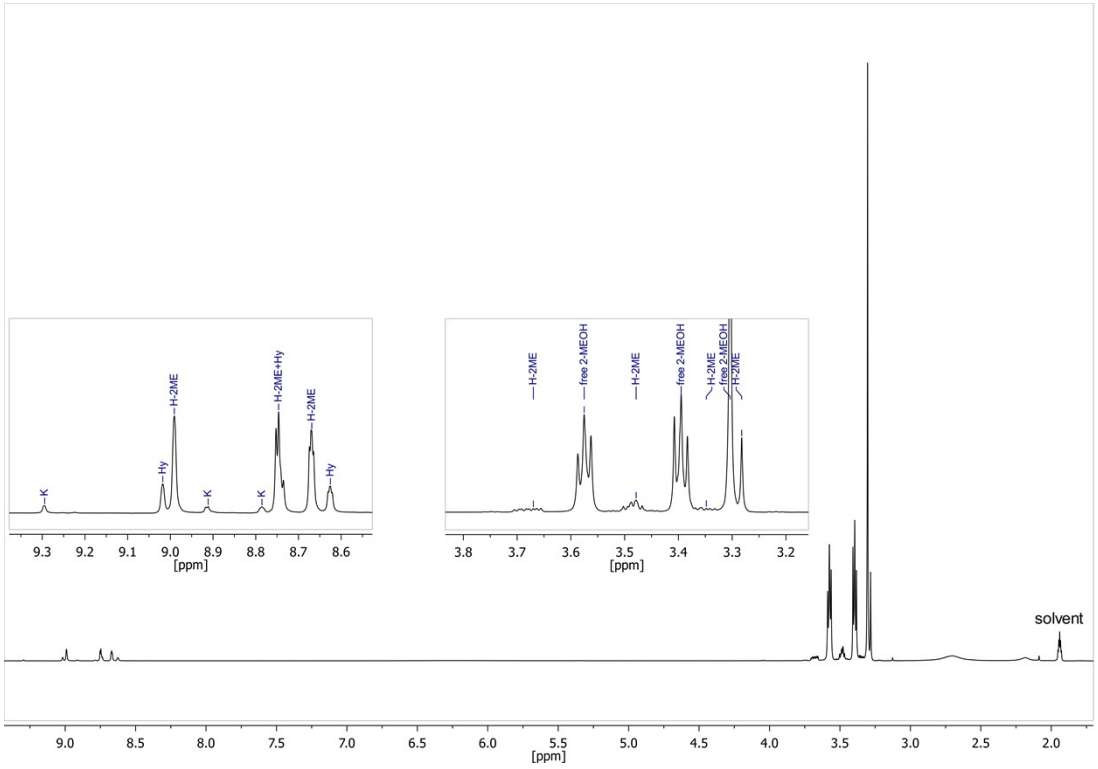

Figure S10 ^{1}H NMR spectrum (298 K) of the 2-ME-dynamic system (using 6 eq. of 2-MEOH) in CD_3CN. H-2ME = 2-methoxyethyl hemiacetal; K = ketone; Hy = hydrate.

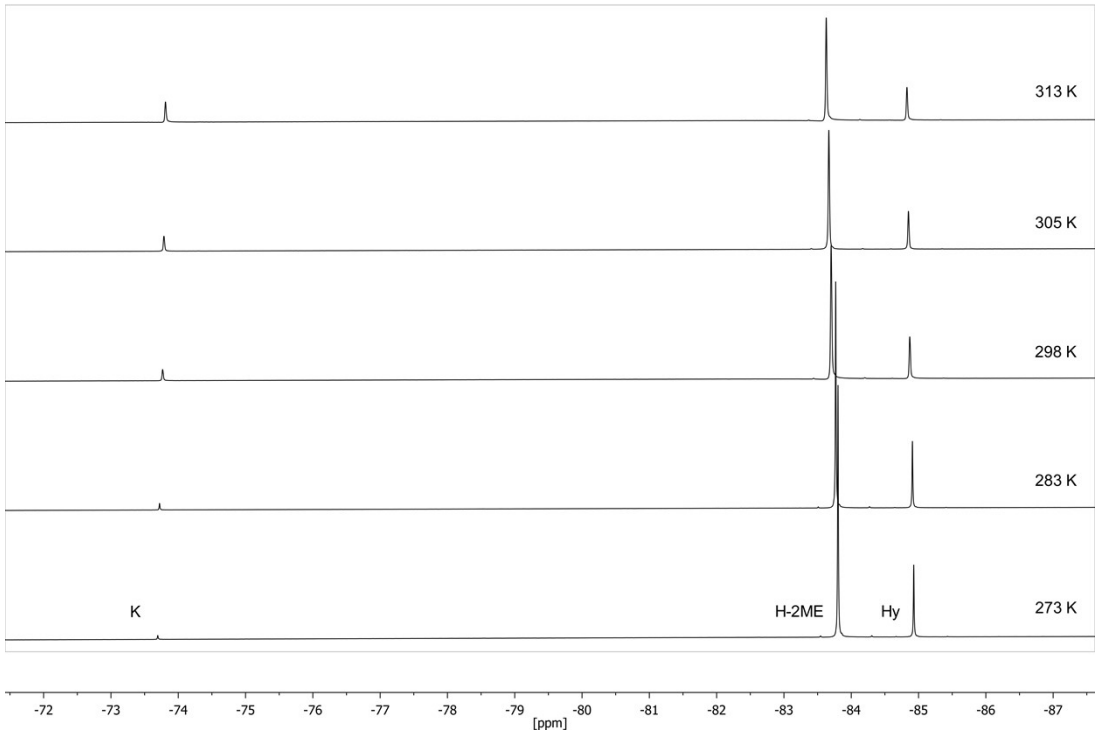

Figure S11 Temperature-dependent ^{19}F NMR spectra of the 2-ME-dynamic system (using 6 eq. of 2-MEOH) in CD_3CN. H-2ME = 2-methoxyethyl hemiacetal; K = ketone; Hy = hydrate.

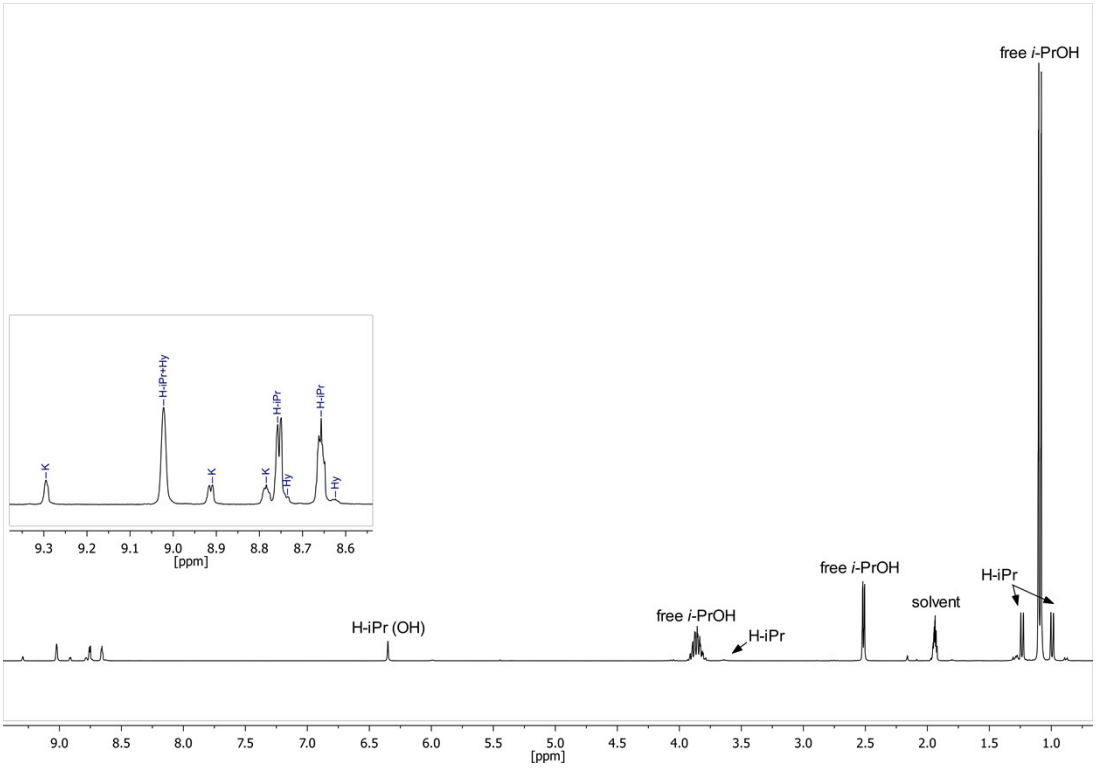

Figure S12 ^{1}H NMR spectrum (298 K) of the H-iPr-dynamic system (using 6 eq. of *i*-PrOH) in CD_3CN. H-iPr = isopropyl hemiacetal; K = ketone; Hy = hydrate.

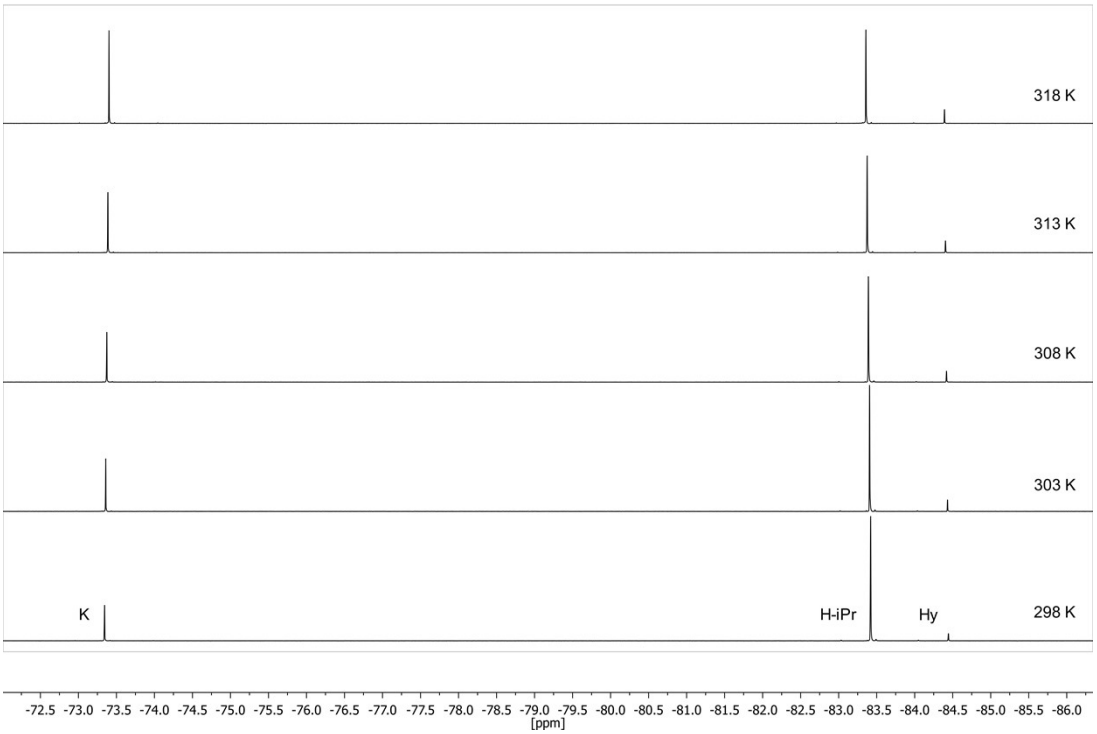

Figure S13 Temperature-dependent ^{19}F NMR spectra of the H-iPr-dynamic system (using 6 eq. of *i*-PrOH) in CD_3CN. H-iPr = isopropyl hemiacetal; K = ketone; Hy = hydrate.

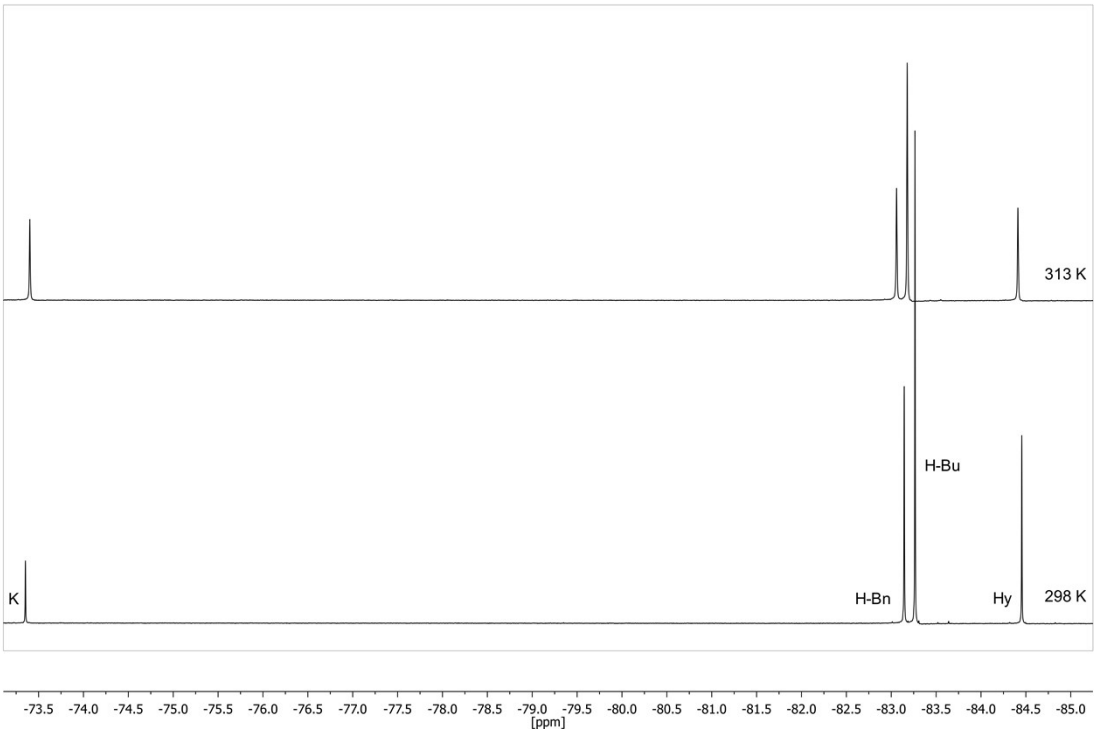

Figure S14 ^{19}F NMR spectra of the mixed H-Bu- H-Bn-dynamic system (using 1.5 eq. of each alcohol) in CD_3CN. H-Bn = benzyl hemiacetal; H-Bu = butyl hemiacetal; K = ketone; Hy = hydrate.

^{13}C NMR spectra

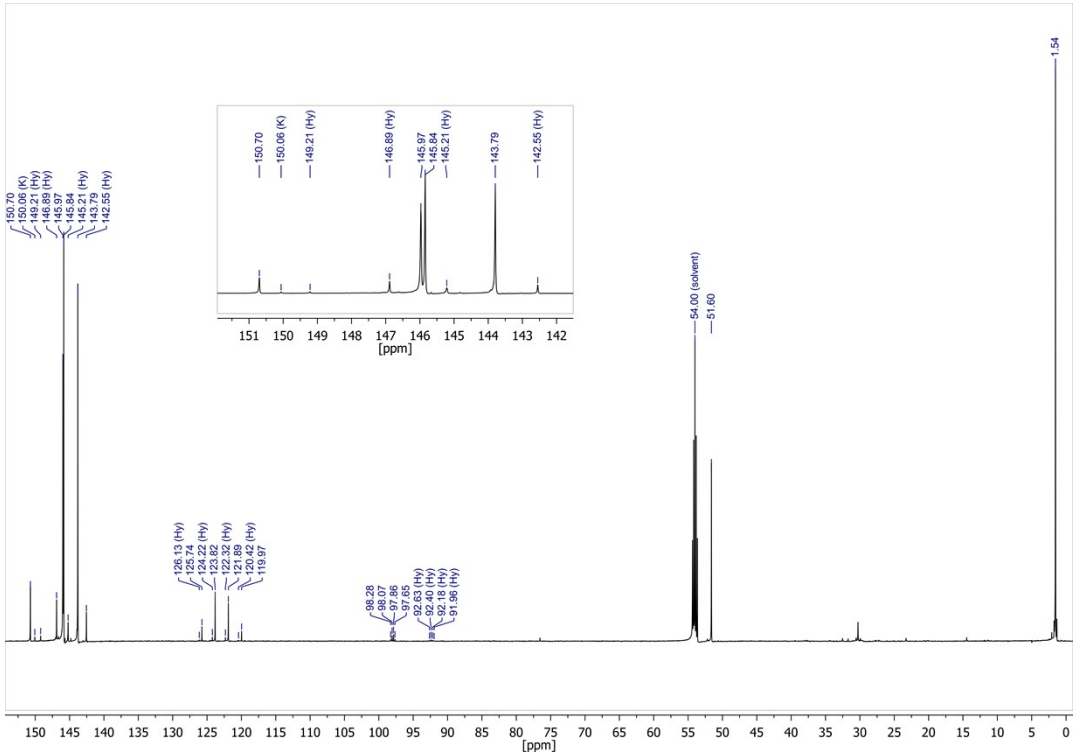

Figure S15 ^{13}C NMR spectrum (298 K) of *O*-silyl ether hemiacetal in CD_2Cl_2. Peaks of the hydrate (Hy) and ketone (K) are visible due to the partial desilylation in NMR solvent.

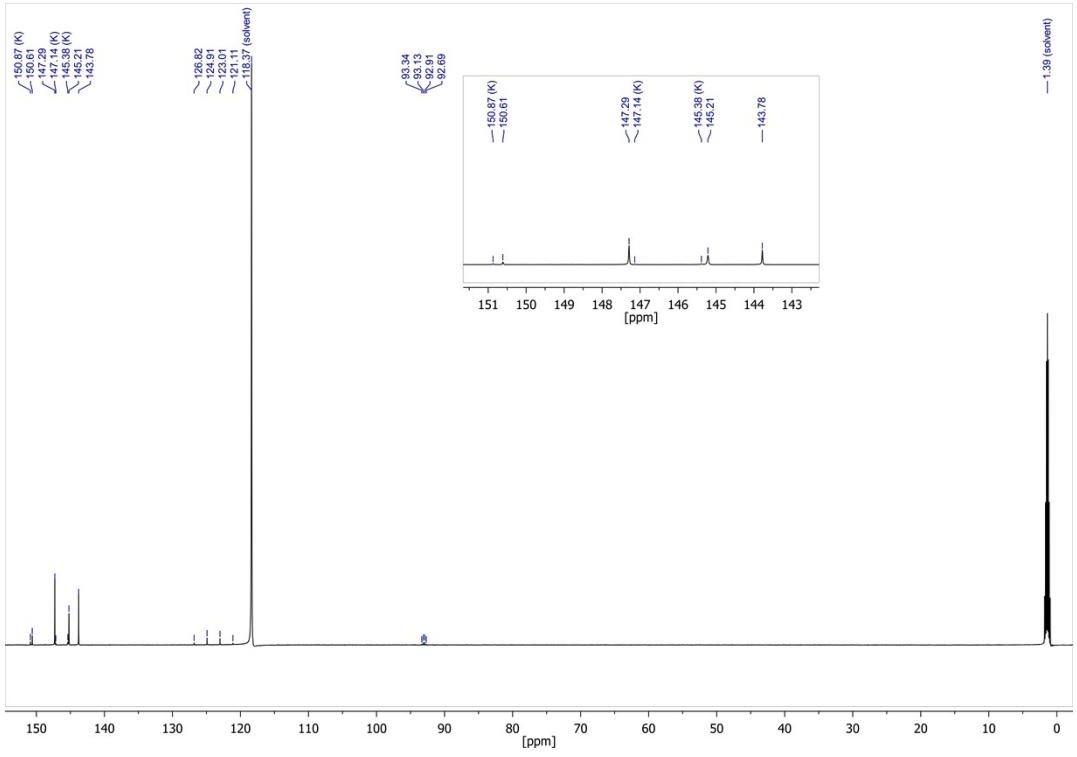

Figure S16 ^{13}C NMR spectrum (298 K) of the hydrate in CD_3CN. K = ketone.

REFERENCES

[1] Sheldrick, G. M. *Acta Crystallogr. Sect. A: Found. Crystollogr.* **2008**, *64*, 112.

[2] SHELXL: Sheldrick, G. M. *Acta Cryst.* **2015**, *C71*, 3.

[3] Spek, A. L. *Acta Cryst.* **2009**, *D65*, 148.

[4] (a) Goodson, P. A.; Oki, A. R.; Glerup, J.; Hodgson, D. J. *J. Am. Chem. Soc.* **1990**, *112*, 6248. (b) Bark, T., PhD thesis, Universität Freiburg (Schweiz), 2004.

[5] Zhao, Y.; Truhlar, D.G. *Theor. Chem. Acc.* **2008**, *120*, 215.

[6] Gaussian 09, RevisionD.01, Frisch, M. J.; Trucks, G. W.; Schlegel, H. B.; Scuseria, G. E.; Robb, M. A.; Cheseman, J. R.; Scalmani, G.; Barone, V.; Mennucci, B.; Petersson, G. A.; Nakatsuji, H.; Caricato, M.; Li, X.; Hratchian, H. P.; Izmaylov, A. F.; Bloino, J.; Zheng, G.; Sonnenberg, J. L.; Hada, M.; Ehara, M.; Toyota, K.; Fukuda, R.; Hasegawa, J.; Ishida, M.; Nakajima, T.; Honda, Y.; Kitao, O.; Nakai, H.; Vreven, T.; Montgomery, J. A., Jr.; Peralta, J. E.; Ogliaro, F.; Bearpark, M.; Heyd, J. J.; Brothers, E.; Kudin, K. N.; Staroverov, V. N.; Kobayashi, R.; Normand, J.; Raghavachari, K.; Rendell, A.; Burant, J. C.; Iyengar, S. S.; Tomasi, J.; Cossi, M.; Rega, N.; Millam, J. M.; Klene, M.; Knox, J. E.; Cross, J. B.; Bakken, V.; Adamo, C.; Jaramillo, J.; Gomperts, R.; Stratmann, R. E.; Yazyev, O.; Austin, A. J.; Cammi, R.; Pomelli, C.; Ochterski, J. W.; Martin, R. L.;Morokuma, K.; Zakrzewski, V. G.; Voth, A.; Salvador, P.; Dannenberg, J. J.; Dapprich, S.; Daniels, A. D.; Farkas, Ö.; Foresman, J. B.; Ortiz, J. V.; Cioslowski, J.; Fox, J. D., *Gaussian*, Inc., Wallingford CT, **2013**.

[7] (a) Fukui, K. *Acc. Chem. Res.* **1981**, *14*, 363. (b) Hratchian, H. P.; Schlegel, H. B. *J. Chem. Phys.* **2004**, *120*, 9918. (c) Hratchian, H. P.; Schlegel, H. B. *J. Chem. Theory and Comput.* **2005**, *1*, 61.

[8] Marenich, A. V.; Cramer, C. J.; Truhlar, D. G. *J. Phys. Chem. B* **2009**, *113*, 6378.

[9] (a) Boys, S. F.; Berdardi, F. *Mol. Phys.* **1970**, *19*, 553. (b) Simon, S.; Duran, M.; Dannenberg, J. J. *J. Chem. Phys.* **1996**, *105*, 11024.

[10] Benjamin P. Pritchard, Doaa Altarawy, Brett Didier, Tara D. Gibson, Theresa L. Windus. *J. Chem. Inf. Model.* **2019**, *59(11)*, 4814.

[11] For 2-methoxyethanol, see: (a) Gil, F. P. S. C.; Amorim da Costa, A. M.; Teixeira-Dias, J. J. C. *J. Phys. Chem.* **1995**, *99*, 16586. (b) Amorim da Costa, A. M.; Duarte, A. S. R.; Amado, A. M. *Vib. Spectrosc* **2006**, *42*, 302. For 1-butanol, see: (c) Ohno, K.; Yoshida, H.; Watanabe, H.; Fujita, T.; Matsuura, H. *J. Phys. Chem.* **1994**, *98*, 6924. For benzyl alcohol, see: (d) Utzat, K.; Restrepo, A. A.; Bohn, R. K.; Michels, H. H. *Int. J. Quantum Chem.* **2004**, *100*, 964. For 2-propanol, see: (e) Kahn, K.; Bruice, T. C. *ChemPhysChem* **2005**, *6*, 487.